Molecular Dynamics Investigation of Charge Carrier Density Influence over Mobility in Conjugated Polymers†

Pedro Henrique de Oliveira Neto, Wiliam Ferreira da Cunha, Ricardo Gargano, and Geraldo Magela e Silva*

Received: May 30, 2009; Revised Manuscript Received: August 07, 2009

Charge carrier mobility is known to be one of the most important efficiency delimiting factors in conducting polymer-based electronic devices. As the transport mechanism in this class of material is nonconventional, many works have tried to elucidate the charge carrier's interaction with temperature, external electric field, and the collective effects they present. Even though the multiple trap-and-release model is often used to describe these effects, its applicability is known to be restricted to electronic properties. In this work we make use of a modified version of the Su−Schrieffer−Heeger model, the most used method to describe the important properties of conducting polymer in general, to investigate the influence of temperature and carrier densities over the transport mechanisms. We obtained different regimes of temperature and carriers density influence over the systems mobility, consistent with most of the experimental data available.

1. Introduction

Due to the advances in the technology of optical electronic conjugated polymer-based devices, such as organic thin-film transistors (TFTs) and organic light emitting diodes (OLEDs), this class of material has attracted great interest from the scientific community.[1−4] Since these electronic devices often present high-field-effect mobility,[5,6] the study of fundamental transport mechanism ought to be elucidated.

One of the most important kinds of charge carrier in conjugated polymers is polarons, a charged half-spin quasiparticle originated from electron phonon coupling. Indeed, polarons are local lattice deformations that polarize neighboring sites as they move. The technological importance of these defects comes from the fact that polarons can respond simultaneously to electric and magnetic fields. In addition, this fact provides a electronic spin resonance (ESR) spectrum to materials having polarons as charge carriers.

To understand the interaction between these unusual charge carriers with their environment and their movement through the molecule chain, many works were done. In an experimental observation Kanemoto et al.[7] investigated the polaron dynamic through electronic spin resonance in two types of iodine-doped long oligothiophenes. In this work it is shown that the increasing temperature reduces the systems anisotropy. Following, in another work Kanemoto et al.[8] obtained a gain of mobility with anisotropy decrease. Matsui and coauthors[9] studied polaron states in high-mobility pentacene TFTs by the same technique. The result was that the single Lorentzian resonance spectra became narrower with higher fields and temperatures. Also, it was observed that greater polarons density is connected with a gain of mobility. These results were explained by multiple trap-and-release (MTR) model, which associates this narrowing with polaron diffusion, thus increasing mobility.

However, MTR model restricts its applicability to electric characteristics only.[10−13] In this sense, a model to describe phenomenologically the charge carriers transport and carriers interaction with temperature, electric field, and themselves is desired. The usual theoretical approach to describe the charge transport in conjugated polymers is the Su−Schrieffer−Heeger (SSH)[14] tight-binding model. In its original fashion, the SSH model does not take these interactions into account, apart from the fact of being the most accepted model to treat conjugated polymers. In the present work we use the SSH model modified to include the action of an external electric field, Brazovskii−Kirova symmetry breaking terms,[15] and temperature effects. In the context of an Ehrenfest molecular dynamics, we performed a numerical simulation of systems with variable charge carrier densities under the action of temperature effects and electric field in the scope of time-dependent unrestricted Hartree−Fock approximation. We obtained the lattice and electron coupled dynamics through the calculation of Euler−Lagrange equations of motion together with time-dependent Schrödinger equations, respectively. The thermal effects were included via a Langevin equation.[16]

Our systems are composed of polyacetylene chains in the cis configuration initially containing different numbers of polarons. Under the action of the external electric field we evaluate the mean velocity of the charge carrier for different temperature regimes. The comparison between these systems results shows that higher temperature regimes are associated with higher charge carrier mean velocity. This result agrees strongly with Chung et al.'s experimental observations.[5] Besides, we observed that the charge carrier density and system mobility are directly correlated, which also agrees with Matsui et al.'s experimental results.[9]

2. Model

We used the following SSH type Hamiltonian:[14]

$$H = -\sum_{n,s} t_{n,n+1}(C^{\dagger}_{n+1,s}C_{n,s} + Hc) + \sum_{n}\frac{K}{2}{y_n}^2 + \sum_{n}\frac{{p_n}^2}{2M}, \quad (1)$$

with $C_{n,s}$ being the annihilation operator of a π-electron with s spin in the nth site. M is the mass of a CH group; K is the harmonic constant; $y_n \equiv u_{n+1} - u_n$, where u_n is the displacement

† Part of the "Vincenzo Aquilanti Festschrift".

10.1021/jp905095a
Published on Web 09/28/2009

coordinate of the molecule site from the completely nondimerized configuration; and p_n is the momentum conjugated to u_n. In the scope of a first neighbor semiempirical tight-binding, $t_{n,n+1}$ is the hopping integral, given by

$$t_{n,n+1} = \exp(-i\gamma A)[1 + (-1)^n\delta_0](t_0 - \alpha y_n) \quad (2)$$

where α is the electron−phonon coupling, t_0 is the transfer integral between the nearest neighbor sites in the undimerized chain, and δ_0 is the Brazovskii−Kirova symmetry breaking parameter. $\gamma \equiv ea/(\hbar c)$, e being the absolute value of the elementar electron charge, c light velocity, and a the lattice constant. The external electric field E was included in terms of the vector potential A, through the Faraday law $E = -(1/c)\dot{A}$. We considered the parameters usually chosen for a polyacetylene chain in cis configuration: $t_0 = 2.5$ eV, $M = 1349.14$ eV $\times$ fs^2/Å^2, $K = 21$ eV A^{-2}, $\delta_0 = 0.05$ and $\alpha = 4.1$ eV A^{-1}. These are values used in theoretical works,[17−19] and we expect the results to be valid for other conjugated polymers as well. This is due to the way our model treats symmetry breaking by changing the amplitude probability of a π-electron bond with different neighbors by the factor δ_0, which is true for almost all conducting polymers

Aspects related to electronic iteraction can be taken into account in the scope of the Hubbard model as adding the SSH Hamiltonian to the following expression

$$H_{\text{Hubb}} = U\sum_i \left(n_{i\uparrow} - \frac{1}{2}\right)\left(n_{i\downarrow} - \frac{1}{2}\right) \quad (3)$$

where $n_{i\uparrow}$ is the number operator for a spin up electron in the nth site and U is the amplitude of the electronic interaction.

To solve the system dynamics, we first prepare a stationary state fully self-consistent with the degrees of freedom of both the electrons and phonons.[20] Then we time evolve the system by finding the following equations for one particle wave functions $\psi_{k,s}$, which are the solutions to the time-dependent Schrödinger equation

$$i\hbar\dot{\psi}_{k,s}(n,t) = -t_{n,n+1}\psi_{k,s}(n+1,t) - t^*_{n-1,n}\psi_{k,s}(n-1,t) + U\left[\rho_{-s}(n,t) - \frac{1}{2}\right]\psi_{k,s}(n,t) \quad (4)$$

where k is the quantum number used to specify each electronic state and the charge densities are defined as

$$\rho_s(n,t) = e\sum{}'\langle\psi_s(n,t)|\psi_s(n,t)\rangle \quad (5)$$

The lattice equation of motion is given by

$$F_n(t) = M\ddot{u}_n = -K[2u_n(t) - u_{n+1}(t) - u_{n-1}(t)] + \alpha[e^{i\gamma A(t)}(B_{n,n+1} - B_{n-1,n}) + e^{-i\gamma A(t)}(B_{n+1,n} - B_{n,n-1})] \quad (6)$$

Here

$$B_{n,n'} \equiv \sum_{k,s}{}'\psi^*_{k,s}(n,t)\,\psi_{k,s}(n',t) \quad (7)$$

is the term that couples the electronic and lattice problems. The primed summation represents a sum over the occupied states only.

We introduce the expansion

$$\psi_k(t) = \sum_l C_{lk}\phi_l(t)$$

with $C_{lk} = \langle\phi_l|\psi_k\rangle$. $\{\phi_l\}$ is the set of eigenfunction while $\{\varepsilon_l\}$ represents the eigenvalues of the electronic part of the Hamiltonian at a given time t.

The obtained solution of the time dependent Schrödinger equation can be written as[16,19]

$$\psi_{k,s}(n,t+dt) = \sum_l\left[\sum_m \phi^*_{l,s}(m,t)\,\psi_{k,s}(m,t)\right]\times \exp\left(-i\frac{\varepsilon_l\Delta t}{\hbar}\right)\phi_{l,s}(n,t) \quad (8)$$

By discretizing the time variable in a small value in the electronic scale, we can solve eqs 4 and 7 numerically.

Temperature effects are included by the use of a canonical Langevin equation. For the fluctuation term we choose a white stochastic signal $\zeta(t)$ with the following properties: $\langle\zeta(t)\rangle \equiv 0$ and $\langle\zeta(t)\,\zeta(t')\rangle = B\delta(t-t')$. A Stokes like dissipation term is also included. Therefore, to include thermal effects in the model we modify eq 6 to

$$M\ddot{u}_n = -\gamma\dot{u}_n + \zeta(t) + F_n \equiv \tilde{F}_n(t) \quad (9)$$

The relationship between ζ, γ, and the temperature T of the system is given by the fluctuation dissipation theorem.

3. Results

The systems are composed of 200 site chains with polarons equally displaced. It is chosen periodic boundary condition to simulate long chains. We present the results of the densities of 6, 9, and 10 polarons per 200 sites. These values were chosen to represent the highest densities observed in TFTs.[9] The simulations took place at temperature regimes of 0, 50, 100, 150, 200, 250, and 300 K. The applied electric field values varied from 1.0×10^{-4} to 2.0×10^{-3} mV/Å.

To visualize the results, we define the charge density order parameter as follows:

$$\bar{\rho}_n(t) = 1 - \frac{\rho_{n-1}(t) + 2\rho_n(t) + \rho_{n+1}(t)}{4} \quad (10)$$

In Figure 1 we present the graphics of the polarons mean velocity as electric field function for all the mentioned temperature in the case of 6 polarons per 200 sites. To calculate mean polaron velocity, we considered the polaron charge center as a function of time and then performed a linear regression. Through the mean angular coefficient calculation, we obtained the velocity in multiples of 30.4 Å/fs. Initially, we observed that at the 0 K regime the velocity is a linear function of the electric field. This is due to the fact that in the absence of thermal perturbation the conductor can be considered ohmic. As the temperature increases, we can observe, for the lower field regimes, a decrease of thermal velocity dependence. This fact

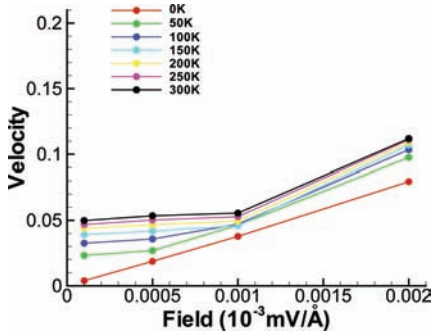

Figure 1. Six polarons per 200 sites: density mean velocity versus field intensity for several temperature regimes.

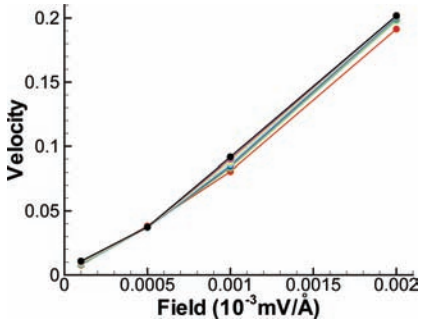

Figure 2. Nine polarons per 200 sites: density mean velocity versus field intensity for the temperature regimes of Figure 1.

is related to the high collision rate of the polarons, which lowers the carriers mean free path. On the other hand, note that the polarons have higher velocities for higher temperatures, referring to the fact that thermal excitation provides energy. It is also worthwhile to emphasize the slight increase of the graphic slope for the highest field. Analogous results were obtained for lower carrier density regimes and are not presented.

Figure 2 represents the same situation for the density of 9 polarons per 200 sites. A remarkable feature of this figure is the near independence of polarons mean velocity with temperature considered in contradiction with the preview case. Observe that for lower electric field the mean polarons velocities approaches the 0 K situation for all temperatures. These conclusions can be explained by the decrease of the intrapolaron space due the higher carrier density. Observe that even for 0 K a non-ohmic behavior is obtained referring to a nonlinear behavior of mobility with polaron density. In this case, it is seen that the mobility is greater compared to the lower carrier density situation. Also, it is noted for higher fields a tenuous temperature dependence of the velocity, which can be visualized by the picture broadening.

The highest carrier density regime considered is presented in Figure 3. This case corresponds to 10 polarons per 200 sites, which is near the saturation density level for TFTs.[9] The figure inset represents just another scale for the velocity. Observe that in this quasi-saturation regime the nonlinear behavior is dominant. We can note that the mobility is much higher than the previous cases. It is important to observe that, while in the other cases the mobility can be considered almost constant, in the present case a strong nonlinear velocity-field dependence occurs. From the inset we notice the increase of velocity-field dependence with temperature. These results are in good agreement with experimental literature.[5,6,9] We can attribute a collective polaron behavior to be responsible for the low and high electric field broadening of the picture.

In Figure 4 we present the graphic of carriers velocity in terms of the polaron number for 0 K. Higher temperature regimes have

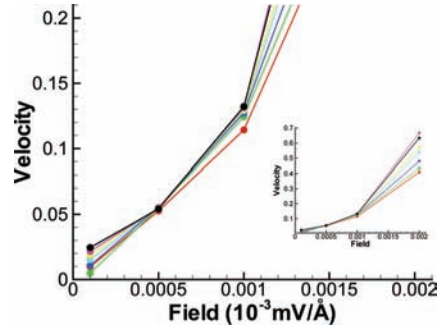

Figure 3. Ten polarons per 200 sites: density mean velocity versus field intensity for the temperature regimes. Inset: same case in a different scale.

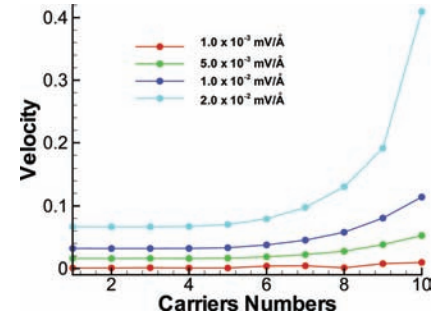

Figure 4. Mean polaron velocity versus polarons numbers per chain for several field intensities at 0 K.

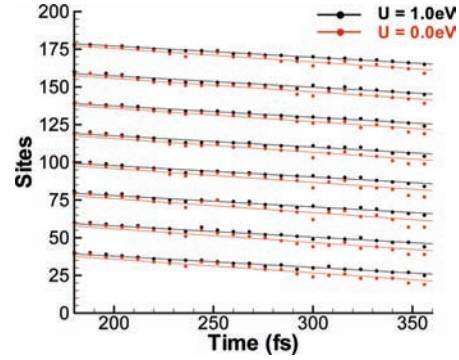

Figure 5. Polaron position as a function of time for different electronic repulsion Hubbard terms $U = 0$ eV (black) and $U = 1$ eV (red).

the effect of raising the polaron velocities for all densities and thus are not shown. Since all simulations were performed with the same chain length, it represents the carrier density per 200 sites in all field regimes. Naturally, for higher fields we have greater polaron mean velocity, which can be seen by the height differences in the curves. Observe that from the first case on the system responds nonlinearly with a further increase of field intensity. The fact of the increase of carrier densities to nonlinearity improves the dependence of velocity with field, i.e., the system mobility. Together with the fact that the collective polarons behaviors help the system mobility dependence with temperature, this elucidates the origin of the high-field-effect mobility in conjugated polymer-based TFTs.

The last set of simulations presented consists of including an on-site Coulomb repulsion approximation in the scope of the Hubbard model. The amplitude of the interaction was chosen according to 15. Figure 5 shows a comparison between the simulations with and without Coulomb interaction. We present a simulation composed of 10 polarons in a 200 site chain under a 300 K temperature regime. It is important to note that this case consists of the highest density polaron regime, where

Coulomb interactions are bigger. The choice of parameter was $U = 1$ eV in eq 3, which is the order of magnitude of the value used in other theoretical works.[15] Each point of the figure represents the position of the polaron center of charge as a function of time. For better visualization purposes, only eight polarons are shown in the figure. It can be seen that the slopes are very similar. From this fact we conclude that electron correlation nearly does not affect the qualitative feature of polaron motion. Quantitatively speaking, it is observed that the simulation subjected to electronic interaction is associated with the lowest mobility in the highest charge carrier density regimes. As far as electronic repulsion being simulated in the Hubbard model, this result is the one expected, because this approximation tends to narrow the charge carrier, thus diminishing its mobility. It is important to note that all the previous simulations were performed with and without the Hubbard interaction term. The presented situation was chosen because it presented the higher difference between both cases. Even in this case the mobility loss is not appreciable, from which we conclude that a reasonable good qualitative result can be achieved even not considering electronic correlation.

4. Conclusions

The influence of the density of charge carriers on conjugated polymer mobility is determined with molecular dynamics calculations. Specifically, we numerically simulated a cis polyacetylene chain containing different quantities of polarons under the action of an external electric field and temperature. To do so, we used a version of the SSH model extended to include these effects. In the context of the Ehrenfest molecular dynamic, we performed the lattice motion through Euler−Lagrange equations simultaneously with the time dependent Schrödinger equation for π-electron motion. Different temperatures, electric field regimes, and polaron densities were considered in this work. We concluded, in agreement with experimental evidence, that thermal effects are directly connected with carrier velocity. An investigation of electron correlation was also performed. From this consideration we concluded that although electronic correlation is important to a precise description of polaron motion, useful qualitative aspects can be obtained from an independent electron model. Another important feature is that the charge carrier density dependence of mobility is shown to be strongly nonlinear. These effects come from the different accommodation patterns the polarons have to face when high-density regimes are concerned. As a consequence, collective effects take place, making the system behave this way, in accordance with experimental results.

Acknowledgment. We are deeply grateful to Prof. Vincenzo Aquilanti for the enlightening discussions throughout contributions to our academic life and scientific view of the world.

References and Notes

(1) Sterpone, F.; Bedard-Hearn, M. J.; Rossky, P. J. *J. Phys. Chem. A Lett.* **2009**, *113*, 3427.
(2) Huang, J.; Wu, Y.; Fu, H.; Zhan, X.; Yao, J.; Barlow, S.; Marder, S. R. *J. Phys Chem. A* **2009**, *113*, 5039.
(3) Neese, B.; Chu, B.; Lu, S.-G.; Wang, Y.; Furman, E.; Zhang, Q. M. *Science* **2008**, *321*, 821.
(4) Huo, F.; Zheng, Z.; Zheng, G.; Giam, L. R.; Zhang, H.; Mirkin, C. A. *Science* **2008**, *321*, 1658.
(5) Chung, D. S.; Lee, D. H.; Yang, C.; Hong, K.; Park, C. E.; Park, J. W.; Kwon, S. *Appl. Phys. Lett.* **2008**, *93*, 033303.
(6) Fumagalli, L.; Binda, M.; Natali, D.; Sampietro, M.; Salmoiraghi, E.; Gianvincenzo, P. D. *J. Appl. Phys.* **2008**, *104*, 084513.
(7) Kanemoto, K.; Furukawa, K.; Neigishi, N.; Aso, Y.; Otsubo, T. *Phys. Rev. B.* **2007**, *76*, 155205.
(8) Kanemoto, K.; Muramatsu, K.; Baba, M.; Yamauchi, J. *J. Phys. Chem. B* **2008**, *112*, 10922.
(9) Matsui, H.; Hasegawa, T.; Tokura, Y. *Phys. Rev. Lett.* **2008**, *100*, 126601.
(10) Calhoun, M. F.; Hsieh, C.; Podzorov, V. *Phys. Rev. Lett.* **2007**, *98*, 096402.
(11) Podzorov, V.; Menard, E.; Rogers, J. A.; Gershenson, M. E. *Phys. Rev. Lett.* **2005**, *95*, 226601.
(12) Carbone, A.; Kotowska, B, K.; Kotowski, D. *Phys. Rev. Lett.* **2005**, *95*, 236601.
(13) Lang, D. V.; Chi, X.; Slegrist, T.; Sergent, A. M.; Ramirez, A. P. *Phys. Rev. Lett.* **2004**, *93*, 086802.
(14) Heeger, A. J.; Kivelson, S.; Schrieffer, J. R.; Su, W. P. *Rev. Mod. Phys.* **1988**, *60*, 781.
(15) Lima, M. P.; e Silva, G. M. *Phys. Rev. B* **2006**, *74*, 224304.
(16) Cunha, W. F.; Neto, P. H. O.; Gargano, R.; e Silva, G. M. *Int. J. Quantum Chem.* **2008**, *108*, 2448.
(17) An, Z.; Wu, C. Q.; Sun, X. *Phys. Rev. Lett.* **2004**, *93*, 216407.
(18) Meng, Y.; Di, B.; Liu, X. J.; An, Z.; Wu, C. Q. *J. Chem. Phy.* **2008**, *128*, 184903.
(19) Neto, P. H. O.; Cunha, W. F.; Gargano, R.; e Silva, G. M. *Int. J. Quantum Chem.* **2008**, *108*, 2442.
(20) Pinheiro, C; da, S.; e Silva, G. M. *Phys. Rev. B* **2002**, *65*, 094304.

JP905095A